Spectral Properties of Spirooxazine Photochromes: TD-DFT Insights

Aurélie Perrier,*,† François Maurel,† Eric A. Perpète,‡ Valérie Wathelet,‡ and Denis Jacquemin*,‡

Laboratoire Interfaces, Traitements, Organisation et Dynamique des Systèmes (ITODYS), CNRS UMR 7086, Université Paris 7—Paris Diderot, Bâtiment Lavoisier, 15 rue Jean Antoine de Baïf, 75205 Paris Cedex 13, France, and Unité de Chimie Physique Théorique et Structurale (UCPTS), Facultés Universitaires Notre-Dame de la Paix, rue de Bruxelles, 61, B-5000 Namur, Belgium

Received: July 22, 2009; Revised Manuscript Received: September 5, 2009

A large series of photochromes of the spirooxazine family has been investigated using density functional theory and time-dependent density functional theory, aiming at designing molecules with an open-ring merocyanine form absorbing at the longest possible wavelength. A complete methodological assessment (basis set, solvent effects, functionals) has been performed, allowing the design of efficient multilinear regressions for two solvents (cyclohexane and toluene). These regressions allow the estimate of the absorption wavelength of open spirooxazine with an error limited to about 5 nm. The thermodynamic and spectral properties of several isomers have been considered, and it turned out that only TTC and CTC structures may appear experimentally. These structures present similar stabilities and absorption wavelengths. The impact of the auxochromic groups on the UV/vis spectra was assessed and novel promising substitution patterns have been unravelled. It is shown that using a strong push moiety on the same side of the molecule as the pull group may be an effective procedure for tuning the visible spectra. In particular, several spirooxazines with absorption wavelength predicted to be close to or larger than 700 nm are proposed.

Introduction

Spirooxazine (SPO, molecules **I**−**III** in Figure 1) derivatives show photochromism, which is defined as the reversible transformation induced by electromagnetic irradiation between two isomers having different properties, notably their absorption spectra and conducting properties.[1] SPO are composed of two heterocyclic fragments, an indoline part and a naphthooxazine moiety, linked through a sp^3 carbon atom (molecule **I** in Figure 1). The spirocyclic form of these compounds absorbs in the UV region. The cleavage of the relatively weak linking between the sp^3 carbon atom and the oxygen atom by UV irradiation is followed by isomerization, which leads to the flattened ring-opened colored isomers, the so-called photomerocyanines. The ultrafast ring-opening reaction can lead to eight different isomers. As illustrated in Figure 2, each isomer corresponds to a given configuration of the molecular fragments relative to the two double bonds (cis, C and trans, T) and the central bond which is partially double (*s*-cis, C and *s*-trans, T). SPO isomers are generally labeled by a three-letter code: the all cis geometry corresponds, for instance, to the CCC isomer. From ^{1}H NMR spectroscopy[2] and resonance Raman spectroscopy,[3] it has been shown that the ring-opening reaction results in the formation of only two merocyanine isomers, TTC and CTC. This finding is in agreement with theoretical predictions that proved that all other isomers are significantly less stable.[4] The reverse ring-closure reaction occurs through a thermal process, the decay of the colored form taking place at the time scale of seconds to minutes at room temperature.[5]

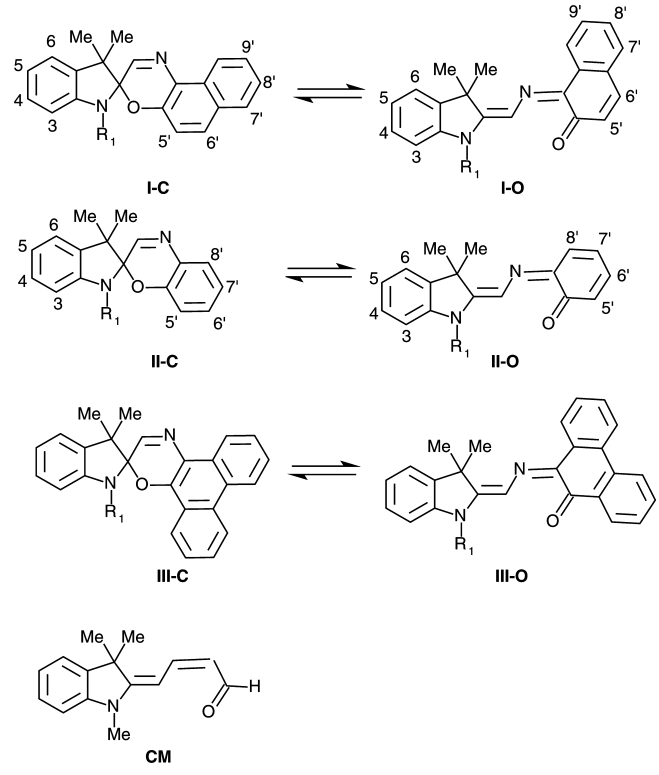

Figure 1. Sketch of investigated photochromes.

Because of their good photochromic and fatigue resistance properties,[6−10] SPO are currently used in many commercial applications, such as sunglasses or ophthalmic lenses, and are considered as promising candidates for memories and switches. Nevertheless, the possible application of SPO in photonic and optical communications[11] requires the development of SPO

* To whom correspondence should be addressed. E-mail: aurelie.perrier-pineau@univ-paris-diderot.fr (A.P.) and denis.jacquemin@fundp.ac.be (D.J.).
† Université Paris 7—Paris Diderot.
‡ Facultés Universitaires Notre-Dame de la Paix.

10.1021/jp906936p CCC: $40.75
Published on Web 09/30/2009

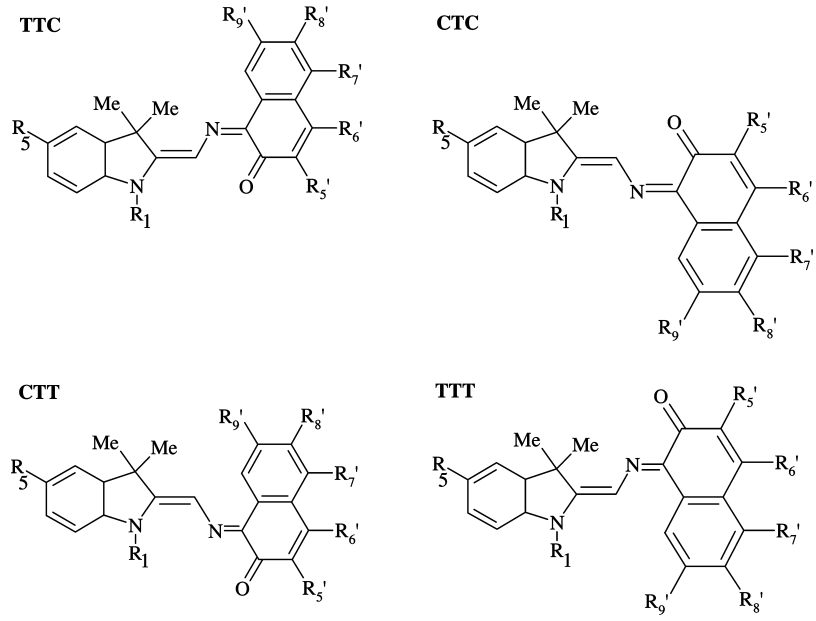

Figure 2. Scheme of the different *s-trans*-merocyanine isomers.

molecules with colored form absorbing as close as possible from the IR region. The design of such photochrom remains a major scientific challenge today.

Using SPO molecules in variable optical transmission materials demands a fine control of both their photochromic and spectroscopic properties. To determine which SPO may be the optimal candidate in a particular device, it is necessary to understand the influence of the molecular structure on the optical and thermodynamic properties of both forms of the photochromic equilibrium. To tackle this task, the relationship between the structures of SPO and their properties as well as the characteristics of thermal and photoinduced processes has been treated in several extensive experimental studies.[12−15] Among different substituted open-ring isomers, a maximum absorption wavelength of 647 nm in cyclohexane[13] has been obtained for a push−pull compound, i.e., electron-donating substituent in the indolinic part (OMe at R_5) and electron-withdrawing substituent in the naphthooxazine part (CN at $R_{6'}$) of the molecule.

To screen and design SPO molecules with open-ring maximum absorption shifted to longer wavelength, quantum chemical calculations are certainly efficient tools. In particular, ab initio calculations, by giving a reliable interpretation of the substituent effects, can predict the optical properties of molecules and orientate the synthesis toward the most promising compounds. So far, despite their potential applications, few theoretical studies have been made on the SPO series. Calculations focusing on the relative thermodynamic stabilities of the four *s*-trans photomerocyanine isomers[16,17] and on the complete description of ground-state ring-opening/closing and isomerization processes[18] can be found. Concerning the optical properties, the accurate prediction of the UV/vis spectra of SPO is still only partially resolved. So far, the maximum absorption wavelength of photomerocyanines were only calculated by using the CS-INDO-CIPSI method.[19] These semiempirical calculations were found to be in reasonable agreement with experimental data, providing the geometry selected is computed at the density functional theory (DFT) level. The improvements in CPU resources now allow the study of the absorption spectra of large molecules with ab initio approaches. Consequently, a huge number of time-dependent DFT (TD-DFT) applications can be found in the literature,[20−23] notably for spiro and diaryl photochromes.[24−27]

This work aims at setting up a TD-DFT scheme able to efficiently predict the maximum absorption wavelength of SPO derivatives. Starting from 1,3,3-trimethylspiro[indoline-2,3′-naphtho[2,1-*b*][1,4]oxazine] (**I-C** with R_1 = Me in Figure 1) as the reference molecule, the calculation scheme should reproduce the substituent effects on the spectral properties in solution. This scheme will then be used to design SPO derivatives with open-ring merocyanine form absorbing at the longest possible wavelength.

Computational Details

In order to simulate the spectral properties of the investigated photochromes, we rely on our well-established three-step methodology (see ref 23 and references therein): (i) the ground-state geometry of each structure has been fully optimized with DFT until the residual mean force is smaller than 1.0×10^{-5} au; (ii) the vibrational spectrum is analytically determined at the same level of theory to confirm that the optimized geometries actually correspond to true minima of the potential energy surface; and (iii) the vertical transition energies to the valence excited states are computed with TD-DFT, which, as noted in the Introduction, is the most popular tool for simulating the excited-states of large molecular systems.[21,23,28,29] For all calculations, a tightened self-consistent field convergence threshold (at least 10^{-8} au) has been applied. As, to the best of our knowledge, no previous extensive TD-DFT investigation has been carried out for the SPO derivatives selected here (see Introduction), we have tested a large panel of atomic basis set for all steps, aiming at determining the atomic functions necessary to obtain fully converged results (see the next section). It turned out that for steps i and ii, a triple-ζ polarized basis set, namely 6-311G(d,p), delivers accurate geometrical parameters, while for step iii, a more extended basis set, 6-311+G(2d,p), has to be used to obtain converged transition wavelengths. The force minimization procedures have systematically used the PBE0 functional[30,31] that delivers accurate ground-state structures for most organic systems.[23] For the TD-DFT part, no investigation indicated the most appropriate functional for this class of compounds, and

we have therefore tested several pure and hybrid functionals: PBE,[32] TPSS,[33] TPSSh,[34] O3LYP,[35] B3LYP,[36,37] PBE0,[30,31] M05,[38] BMK,[39] BHandHLYP,[40] and M05-2X.[41] These functionals cover a large range of exact exchange percentage (from 10% for TPSSh to 56% for M05-2X) and offer a representative set of possible TD-DFT schemes.

The bulk solvent effects were evaluated by means of the well-known polarizable continuum model (PCM).[42] In PCM, the solvent is treated as a structureless medium presenting characteristics matching the experimental physical constants of the environment. Consequently, PCM returns a valid approximation of solvent effects as long as no specific interactions link the solute and the solvent molecules. For this reason, we have mainly simulated experiments carried out in the aprotic cyclohexane (CH) and toluene (Tol) media, though some test calculations with protic solvents, such as ethanol (EtOH), have also been performed. As we model absorption spectra, we have systematically used the nonequilibrium PCM model for TD-DFT calculation,[43] since the absorption processes typically present short characteristic times.

To improve the agreement between theory and experiment, statistical corrections can be useful. In addition to standard linear regression (SLR, simple linear regression), we have also carried out multiple linear regression (MLR) that is able to advantageously combine the results generated by several theoretical approaches. Here, we have used the MLR implementation available in the StatGraphics package.[44] Such technique has been successfully used to predict the λ_{max} of anthraquinone dyes.[45−47]

Eventually, we can briefly list the limitations of our computational scheme. Aside from the approximation inherent to the use of approximate exchange-correlation functionals, the most important for comparisons with experimental UV/visible spectra is certainly the lack of vibronic couplings in our model, though some SPO have a clear vibronic signature.[12] It is well-known that the difference between the 0−0 and vertical transition is on the order of 0.1−0.3 eV.[22,48] Unfortunately, while TD-DFT calculations of the Franck−Condon factors exist,[49,50] they are in practice unfeasible for the extended set of large solvated chromogens considered herein. Another limitation of our approach is that the surface charges of the PCM cavity are optimized for the ground state, not for the excited state. Unfortunately, we do not have access to computer codes implementing the so-called state-specific approximation[51] that solves this problem.

Methodological Investigation

Basis Set and Solvent Effects. Tables, available in Supporting Information, list the wavelengths computed for the two first transitions of the model **II** (R_1 = Me) in both open and closed forms. In this model, the replacement of the naphtooxazine moiety by a benzooxazine cycle should reproduce the influence of the basis set on the geometrical and optical properties of the model **I** SPO. The simplification of the structure decreases the computational cost and therefore allows us to test a large panel of basis sets for both open- and closed-ring forms. For the open form, one systematically finds a first dipole-forbidden $n \rightarrow \pi^*$ transition corresponding to the promotion of an electron from the HOMO-1 to the LUMO (see Figure 3) and a second strongly allowed $\pi \rightarrow \pi^*$ band that is related to an HOMO to LUMO transition. For the closed-ring form, the two first transitions are allowed, though they present relatively small oscillator strengths: the longest (shortest) wavelength transition being related to a HOMO to LUMO (HOMO-1 to LUMO) electron promotion inducing a significant (almost no) charge transfer from the two sides of the molecule, as can be seen in Figure 3. As we aim at finding the appropriate combination providing converged λ_{max}, we have selected a large panel of basis sets for the geometry optimizations: 6-31G, 6-31G(d,p), 6-311G(d,p), 6-311++G(d,p), 6-311G(2d,2p), 6-311+G(2d,p), and 6-311++G(2d,2p), as can be seen in Table S1 (Supporting Information). For the TD-DFT part, in addition to the same list of basis sets, 6-31G(d), 6-31+G(d), 6-31++G(d,p), 6-311+G(d), 6-311+G(2df,2p), and 6-311++G(2df,2pd) have also been tested. This investigation has been performed in the gas phase using the PBE0 functional, as the choice of a specific functional or the inclusion of solvent effects have little impact on the relative modifications induced by the basis set (though they can certainly tune the absolute transition energies). Let us first compare the wavelengths computed with different "TD-DFT basis sets" on a given geometry, namely, the PBE0/6-311++G(2d,2p) one. For the open form, the second ($\pi \rightarrow \pi^*$) transition, which is of interest for the design of new photochromic structures, is located at 486 nm by the largest basis sets. To obtain any reasonable estimate of this value, the inclusion of both diffuse and polarization orbitals is mandatory, at least for second-row atoms. Indeed, the λ_{max} is 460 nm with 6-31G, 470 nm with 6-31G(d,p), but 480 nm with 6-31+G(d). Obviously, the values are only fully converged with the 6-311+G(2d,p) basis set: we select this basis set in the following, as it also yields converged transition energies for both peaks of the closed form. The same basis set has been shown to be appropriate for other classes of delocalized photochromic structures.[24,52,53] For the $n \rightarrow \pi^*$ transition of the open structures (of limited interest for our purposes), the basis set sensitivity is so large that the addition of f polarization orbitals are required to obtain full convergence. The fact that very large basis sets may be mandatory to reach convergence for $n \rightarrow \pi^*$ transitions has already been noticed previously for other chromogens.[54,55] The impact of modifying the basis set used during the geometry optimization procedure is unsurprisingly smaller: 6-311G(d,p) is sufficient to obtain wavelengths within 1 or 2 nm of that of a (much) larger basis set, for both transitions of both forms. As

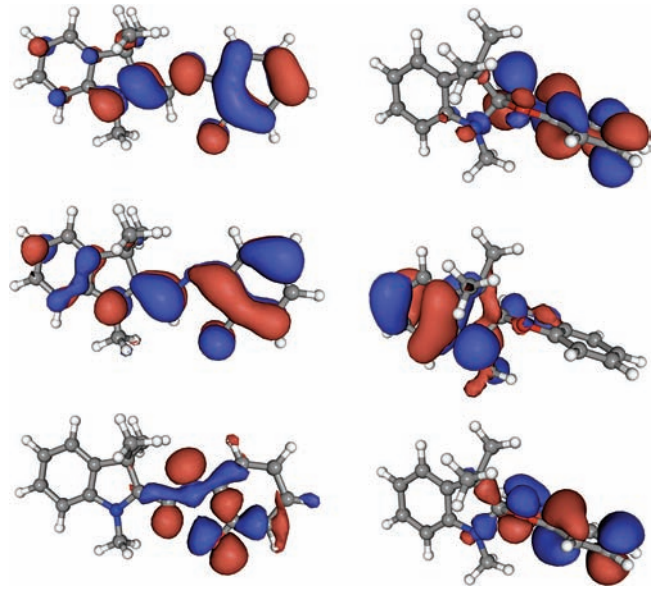

Figure 3. Relevant molecular orbitals for the open (left) and closed (right) model **II** structures used in the benchmark calculations. From top to bottom: LUMO, HOMO, and HOMO-1. The contour threshold is set to 0.03 au, and these orbitals have been computed at the PCM(Tol)-PBE0/6-311+G(2d,p)//PCM(Tol)-PBE0/6-311G(d,p) level of approximation.

shown in Table S2 (Supporting Information), the same basis set also delivers relative stabilities for the open- and closed-ring forms that are very close to the values obtained with the largest basis sets. For instance, the ΔH (ΔG) is −11.16 (−8.82) kcal mol^{-1} with 6-311G(d,p) and −11.42 (−9.02) kcal mol^{-1} with 6-311++G(2d,2p). Consequently, we will stick to a 6-311+G(2d,p)//6-311G(d,p) approximation in the following. Using a smaller basis set in the DFT and TD-DFT calculations could induce a small but non-negligible bias. This is illustrated by the effective optical contrast between closed and open forms that is 129 nm with the largest basis sets but 117 nm with 6-31G(d,p), an error of 9%.

In Table S3 (Supporting Information), we present the importance of modeling the surrounding solvent by considering separately the *direct* (on the absorption spectra) and *indirect* (on the geometry) effects. It turns out that one must include the PCM model during the TD-DFT calculations, as it strongly modifies the transition energies, especially in the open form. Indeed, for this structure, it leads to a hypsochromic displacement (ca. −15 nm) for the $n \rightarrow \pi^*$ band but a bathochromic displacement (ca. +25 nm) for the $\pi \rightarrow \pi^*$ transition. As the effects are smaller for the closed compounds, the absorption wavelength contrast is slightly increased by the inclusion of bulk solvent effects. The indirect effect, while significantly smaller, remains nontrifling. Therefore, all calculations including geometry optimization and Hessian calculations systematically include the PCM model in the following.

Choice of a Functional. In Tables S4 and S5 (Supporting Information), we present the results obtained with 10 different functionals as well as with the TD-HF approach and compare them to experimental values for a large set of derivatives of type **I** in cyclohexane and toluene, respectively. As our primary focus of the present investigation is to increase the absorption wavelength of open SPO photochromes, we have not considered the closed form in this initial investigation. Moreover, we assume that the impact of the auxochromic groups is less important on the UV/vis spectra of the colorless closed-ring isomers than on the colored open-ring one, a common feature of photochromic molecules.[25] From Table S4 (Supporting Information), it is obvious that pure functionals provide λ_{max} closer to experiment than other approaches, all hybrids tending to underestimate significantly the absorption wavelength. This is illustrated by the unsubstituted compound with an error of 39 nm for PBE, but 70 nm for B3LYP and 97 nm for M05-2X. It is well-documented that TD-B3LYP provides too large transition energies for similar (mero)cyanine derivatives.[27,56] This large error of the hybrids is reflected in the mean signed error (MSE, experiment − theory) and mean absolute error (MAE) at the bottom of Table S4 (Supporting Information) that lie in the 50−100 nm range, i.e., that are much larger than the usually expected TD-DFT discrepancies.[23,57] More important for practical design of new photochromic units are the relative values: which functional is able to best simulate the auxochromic shifts? A nitro group at R_5 experimentally induces an hypsochromic displacement of −41 nm, a shift very poorly estimated by the two pure functionals that predict large bathochromic displacement: PBE (+77 nm) and TPSS (+73 nm). The absolute error with hybrids is smaller (e.g., B3LYP: +24 nm) but still provides the wrong sign, but for BHandHLYP and M05-2X for which a constant absorption wavelength is foreseen. In fact only TD-HF yields the most reasonable estimate (−14 nm). Another example is the difference between the unsubstituted molecule and the strong push−pull derivative (R_5 = OMe, $R_{6'}$ = CN), which reaches +69 nm experimentally, +81 nm with PBE, +59 nm with B3LYP, +56 nm with PBE0, and +39 nm with HF. In other words, pure functionals overestimate the auxochromic displacement, hybrids provide close estimates, and HF underrates the shift. The same conclusion holds for most refined effects. For instance, the difference between the R_5 = OMe, $R_{6'}$ = CN, and R_5 = OMe, $R_{8'}$ = CN derivatives, +35 nm experimentally, is estimated to be +41 nm with PBE, +35 nm with B3LYP, +33 nm with PBE0, and +20 nm with HF. Therefore, while hybrids provide large MAE, they tend to deliver reliable auxochromic displacements.

Of course, one may believe that the recently developed range-separated hybrids (RSH)[58−62] would be more suited for these strongly delocalized excited-states. However, the investigated molecules present a strong cyanine character, and we have demonstrated[56] that, in this specific case, RSH do not improve (nor worsen) the estimates of conventional hybrids. The errors are indeed related to the multideterminantal nature of the ground state of such chromophores.[63] For a model system (**CM** in Figure 1), (14,13)-CASSCF/6-31G(d) calculations confirm the multideterminantal nature of the wave function, which is a combination of three major configurations with determinants weights of 0.89, −0.13, and −0.12. This is a quite remarkable result as the naphthalene moiety on the right-hand side of the molecule has been neglected, though it could be foreseen that this chemical group could boost the multideterminantal character. For the record, the configuration with a −0.13 weight corresponds to a structure with the opposite single/double bond pattern and is related to a double excitation, whereas the third configuration arises from double electronic excitation localized on the phenyl ring. Unlike (TD-)DFT, CASSCF calculations can correctly describe SPO as a superposition of zwitterionic and quinoidic structures.[4] We are therefore on the horns of a dilemma: CASSCF provides a more chemically sound ground state (but extremely poor transition energies), CAS-PT2 estimates are practically unfeasible for the actual systems of interest, and TD-DFT is bonded to deliver inaccurate wavelengths. Therefore, as we aim at an effective compromise between computational cost and accuracy, we perform statistical corrections of the TD-DFT values in the next section.

Results and Discussion

Statistical Model for Calculating the λ_{max}. As seen above, a statistical treatment of the raw TD-DFT data is necessary to obtain accurate evaluations of both the auxochromic displacements and wavelengths. One could think that once statistical corrections are performed, the use of large basis set and inclusion of bulk solvent effects in the model become unnecessary. Unfortunately, this is untrue: for diarylethenes we have shown that the quality of the statistical analysis is dependent on the quality of the TD-DFT input.[26] The SLR results for cyclohexane and toluene are shown at the bottom of Tables S4 and S5 (Supporting Information), respectively, and it turns out that functionals including a larger share of exact exchange tend to deliver the largest correlation coefficients (for instance, in cyclohexane, R^2 = 0.48 for O3LYP, 0.58 for B3LYP, and 0.78 for BHandHLYP). Therefore, PBE and TPSS that provided the smallest MAE prior to statistical corrections are the two most unsatisfactory functionals for fitting. This finding is consistent with the large errors in the auxochromic shifts noted above. While the MAE obtained after SLR can be as small as 9 nm, the obtained correlation coefficients are certainly unsatisfactory. For this reason, we have performed a MLR treatment of the results. After several tests, optimal MLR equations could be identified for cyclohexane and toluene:

$$\lambda^{\text{Exp-Cyclohexane}} = -170.88 - 0.76\lambda^{\text{TPSS}} + 2.55\lambda^{\text{B3LYP}} - 2.89\lambda^{\text{BHandHLYP}} + 2.83\lambda^{\text{HF}} \quad (1)$$

$$\lambda^{\text{Exp-Toluene}} = -57.70 - 0.14\lambda^{\text{PBE}} + 0.24\lambda^{\text{TPSSh}} + 0.38\lambda^{\text{PBE0}} + 0.95\lambda^{\text{HF}} \quad (2)$$

It is worth noting that the notable difference between the two equations describing these apolar solvents relies on a statistical analysis and does not imply any physical interpretation about the reliability of individual functionals. Both equations are quite powerful. Indeed the former (latter) provides a R^2 of 0.91 (0.96), significantly better than any SLR, while the associated MAE is as small as 6 (4) nm. For the record, both equations are statistically significant at the 99% level, while the confidence in each term is higher than 90%. As can be seen from Table 1, eqs 1 and 2 are able to reproduce the three auxochromic displacements mentioned in the previous section: −34 nm (instead of exp −41 nm) for the $R_5 = NO_2$ derivative, +68 nm (instead of +69 nm) for the push−pull effect (OMe at R_5 and CN at $R_{6'}$), and +33 nm instead of +35 nm when moving the cyano group from $R_{8'}$ to $R_{6'}$. For the record, it has been reported previously that the photochromic reaction takes place through a triplet rather than a singlet path for nitro-substituted SPO.[64,65] For this reason, we have checked the nature of the ground state of the $R_5 = NO_2$ structure. It clearly pertains to the singlet family: the most stable triplet geometry appears more than 25 kcal mol^{-1} above the singlet one.

TABLE 1: Comparison between Theoretical and Experimental Wavelengths (in nm) for the λ_{max} of I-O (R_1 = Me)[a]

	cyclohexane		toluene	
substituents	theory, eq 1	experiment	theory eq 2	experiment
	582	578	594	596
R_5 = OMe	593	593	607	612
$R_5 = NO_2$	548	537	586	591
$R_{5'}$ = OH	573	573	618	622
$R_{5'}$ = COOMe	589	596	607	612
$R_{5'}$ = CHO	611	617	627	633
R_5 = OMe, $R_{5'}$ = CH=CHCN	627	632	636	645
$R_{6'} = NC_5H_{10}$	549	543	572	567
$R_{6'} = SO_2$−Ph−Me	626	623	635	638
$R_{6'}$ = CN	636	631	646	645
R_5 = OMe, $R_{6'}$ = CN	650	647	656	661
$R_{8'}$ = Br	591	591	605	608
$R_{8'}$ = CN	602	597	607	611
R_5 = OMe, $R_{8'}$ = CN	617	612	622	622
$R_{8'} = R_{9'}$ = CN	624	612	624	620
$R_{8'}$=NO_2	602	603	612	617
$R_{9'}$ =OMe	586	581	592	595
R_5 = OMe, $R_{9'}$ = OMe	597	593	604	609
$R_{5'} = CH_2OH$	575	591	593	605
R_5 = OMe, $R_{5'} = CH_2OH$	594	623	608	618
$R_{5'}$ = CH=CH−CHO	616	618	629	632
$R_{5'}$ = CH=CHCN	615	615	623	626
$R_{5'} = CH{=}C(CN)_2$	655	658	664	668
$R_{6'}$ = S−Ph−OMe	633	624	637	637
$R_{7'} = NO_2$			600	605
$R_{8'}$ = OMe	594	588	612	608

[a] All calculations have been performed at the PCM-TD-X/6-311+G(2d,p)//PCM-PBE0/6-311G(d,p) level and the results are following MLR fitting (see the text for more details). The experimental values have been taken from several references.[12−15]

In order to validate the MLR equations, we have selected molecules not included in the training set and simulated their absorption wavelength. To make these tests nontrivial, we have used SPO with significantly different nature than those of Table 1. The first is SPO **III-O** (R_1 = Me), in which a phenanthrene replaced the naphthalene part. For this molecule, the experimental λ_{max} is 568 nm in cyclohexane,[12] a value nicely estimated by our scheme: 570 nm. Experiments have also been carried out on cationic SPO.[66,67] In particular, the absorption wavelength of **I-O** (R_1 = Me), in which the CH unit at $R_{7'}$ has been replaced by a NMe^+ group, attains 615 nm in toluene experimentally.[66] This value is very nicely reproduced by eq 2, which delivers a λ_{max} of 619 nm, although no charged SPO was included in our training set. These two examples exemplify the efficiency of the MLR procedure.

Energetic and Spectral Properties of Photomerocyanine Isomers. For the closed form of the unsubstituted compound, XRD measurements are available,[68] and it turns out that PBE0/6-311G(d,p) reproduces the main features of the experimental structures (see Table S6 in the Supporting Information). For instance, the mean absolute deviation for the bond lengths of the two rings connected to the central spiro carbon atom is limited to 0.019 Å, and the typical errors are significantly smaller for the aromatic rings. Likewise, the torsion between the two sides of the molecule is 95.1° experimentally and −92.3° with PBE0. To the best of our knowledge, no successful XRD measurements have been achieved out for the open isomers, because of their unstable nature. Therefore, a comparison between the theoretical and the experimental evolutions of the bond lengths upon ring-opening remains impossible.

As discussed in the Introduction, the possible configurations of the two double bonds (C=C and N=C) and the partial central double bond (C−N) lead to eight distinct isomers for the merocyanines. These conformers have been investigated previously,[4,17] though only unsubstituted molecules have been modeled with less refined theoretical models. Due to the steric hindrance between the naphtooxazine and the indoline moieties, the conformations with a central *s*-trans bond (TTC, CTC, TTT, and CTT) are more stable than their *s*-cis counterparts (TCC, CCC, TCT, and CCT) by at least 10 kcal mol^{-1}.[4] Subsequently, our investigation has been restricted to the *s*-trans derivatives (see Figure 2).

The relative standard enthalpies of these molecules are given in Table 2. The most stable configuration corresponds to the TTC geometry, the CTC isomer being less stable by 1.52 kcal mol^{-1} in the gas phase, whereas the CTT and TTT structures are much more energetic. These results are in agreement with both previous theoretical estimates[4,17] and ^{1}H NMR and resonance Raman measurements.[2,3] Indeed, these low temporal resolution spectroscopies have shown that the ring-opening reaction only yields two isomers, namely TTC and CTC. Table 2 also demonstrates that increasing the solvent polarity does not significantly modify the relative stability of the different isomers. In fact, the inversion of the relative stability of the high-energy isomers (TTT and CTT) in ethanol is the only appreciable qualitative change. The comparison of the relative standard enthalpies of the open-ring TTC and the closed-ring isomer shows that the photochromic equilibrium is shifted to the closed form and that the relative stability of the closed-ring isomer is less pronounced in polar environment. This latest phenomenon is explained by a strong stabilization of the polar TTC and CTC isomers (dipole moments of 4.81 and 5.40 D in CH) in comparison with the closed-ring structure (dipole moment of 1.03 D in CH) and follows the experimental trends.[69]

TABLE 2: Relative Standard Enthalpies ΔH° and Relative Free Energies ΔG° (in kcal mol^{-1}) of the Isomers (see Figure 2) in Different Solvents (CH, cyclohexane; Tol, toluene; Et, ethanol)[a]

		ΔH°						ΔG°					
		open				closed		open				closed	
substituents	solvent	TTC	CTC	TTT	CTT		exp[69]	TTC	CTC	TTT	CTT		exp[69]
	gas phase	0.00	1.52	8.37	7.95	−5.29		0.00	1.77	8.53	8.60	−2.30	
	CH	0.00	1.59	8.08	7.88	−4.41		0.00	1.72	8.05	8.30	−1.70	
	Tol	0.00	1.12	8.01	7.87	−4.23	−5.19	0.00	3.08	7.97	8.21	−1.56	−6.70
	Et	0.00	1.74	7.23	7.74	−2.24	−5.00	0.00	1.58	6.95	7.58	−0.07	−5.41
$R_{6'} = CN$	CH	0.00	1.52	8.45	8.24	−5.11		0.00	1.46	8.38	8.53	−2.67	
$R_5 = NH_2$	CH	0.00	1.42	8.19	7.38	−2.85		0.00	1.42	7.84	8.29	−0.32	
$R_{6'} = CN$, $R_5 = NH_2$	CH	0.00	1.43	8.11	8.48	−3.05		0.00	1.39	10.11	8.80	−0.58	

[a] The TTC conformation is considered as the reference structure. Calculations have been performed at the PCM-TD-PBE0/6-311+G(2d,p)//PCM-PBE0/6-311G(d,p) level.

The calculation nevertheless overestimates the experimentally observed solvatochromic effect, probably due to the existence of specific solute−ethanol interactions that are not accounted for in the PCM model.

The same qualitative conclusions regarding the relative stabilities of the various isomers can be drawn with the free enthalpies, the TTC isomer remaining the most stable in all solvents. From toluene to ethanol, the solvatochromic effect is qualitatively reproduced by calculations: the open ring isomer is experimentally 1.29 kcal mol^{-1} (calc. 1.49 kcal mol^{-1}) more stable in ethanol. The significant difference between the calculated and the measured ΔG° can be explained by PCM restrictions and by experimental limitations. Indeed, according to Favaro et al.,[69] the estimated values of the reaction entropy are on the same order of magnitude as the experimental error.

We have also investigated the influence of the substituents on the relative energies computed in cyclohexane. Adding an electron-withdrawing cyano group at the position 6′ of the naphthalene leads to a stabilization of the closed-ring isomer with respect to the open-ring ones but does not affect the relative stabilities of the different merocyanine isomers. On the contrary, the insertion of the NH_2 electron-donating group at the position 5 of the indoline fragment leads to a destabilization of the closed-ring isomer and to a significant stabilization of the CTT isomer, though this isomer remains 7.38 kcal mol^{-1} over the TTC reference. The stabilization (destabilization) of closed-ring isomer with electron-withdrawing (electron-donating) substituents is in perfect agreement with experimental trends.[12,69] The behavior of the push−pull compound is similar to the molecule substituted with an electron-donating group: the closed-ring isomer becomes relatively less stable.

We have also calculated the spectral properties (λ_{max}) of the four merocyanine isomers in cyclohexane with the MLR eq 1 as well as the PBE0 and BMK functionals. As the MLR equation has been designed for specific isomers, its efficiency for other conformers is doubtful and it was only applied to the TTC structures. For the unsubstituted compound, Table 3 shows that the two most stable isomers present almost perfectly the same maximum absorption band with both functionals. Likewise, for substituted molecules, the difference between the λ_{max} of TTC and CTC isomers remains very small. For both unsubstituted and substituted SPO, the λ_{max} of the more energetic TTT and CTT isomers undergoes a limited bathochromic shift (∼7 nm for TTC and ∼18 nm for CTT). It is worth noting that for CTC structures, PBE0 and BMK calculations show the existence of a (very) weak transition at longer wavelength. This red-shifted peak, which appears only on the CTC spectrum, would probably remain unseen experimentally, as its calculated oscillator strength is on average only one-eighth of the strength of the maximum absorption peak. In most cases, the measured stationary absorption spectra of open-ring SPO molecules present an asymmetrical shape, with a shoulder on the short-wavelength side (more rarely on the long wavelength side).[12] The wavelength difference between the λ_{max} band and the shoulder ranges from 20 to 50 nm. As a consequence, our calculations corroborates the generalized assumption that the asymmetrical shape of the maximum absorption band does not result from the overlapping of TTC and CTC bands but more probably from vibronic couplings. To confirm this hypothesis, calculations of the vibronic coupling of TTC would be needed[49,50] but are beyond the scope of the present study.

TABLE 3: Investigation of the Conformation Effects (see Figure 2) on the λ_{max} (in nm) at the PCM(CH)-TD-X/6-311+G(2d,p)//PCM(CH)-PBE0/6-311G(d,p) Level

substituents		TTC	CTC	TTT	CTT
	MLR, eq 1	582			
	PBE0	500	500, 532 sh	507	518
	BMK	481	479, 497 sh	482	495
$R_{6'} = CN$	MLR, eq 1	636			
	PBE0	540	535, 560 sh	555	564
	BMK	517	527, 502 sh	523	535
$R_5 = NH_2$	MLR, eq 1	606			
	PBE0	527	534, 520 sh	533	542
	BMK	501	506, 483 sh	501	512
$R_{6'} = CN$, $R_5 = NH_2$	MLR, eq 1	668			
	PBE0	572	577, 545 sh	587	594
	BMK	541	545, 499 sh	546	556

Analysis of Auxochromic Effects. In ref 12, it is pointed out that adding an acceptor group on the naphthooxazine side and an donor group on the indoline moiety produces larger absorption wavelength due to the well-known push−pull effect. However, to the best of our knowledge, the substitution effect has not been analyzed systematically previously. For this reason, we assess the impact of the substitution by a donor (NH_2) or an acceptor group (CN) at each possible position, that is, from 3 to 6 on the indoline side and from 5′ to 9′ on the naphtooxazine side (see **I-O** of Figure 1). The results obtained with eq 1, as well as with PBE0, are listed in Table 4. Starting with the MLR reference absorption wavelength at 582 nm for the unsubstituted molecule, it is obvious that the addition of a cyano group on the indoline side tends to decrease the absorption wavelength for all four positions: 3 (−29 nm), 4 (−20 nm), 5 (−20 nm), and 6 (−21 nm). The synthesis of these molecule, a task not performed at the present time, is consequently of little use for our objectives (see Introduction). On the contrary, adding the acceptor group on the naphthooxazine moiety provokes a bathochromic displacement in all cases, though the effect is only trifling for 7′ (+9 nm). The two largest modifications are

TABLE 4: Analysis of the Impact of Substituents on the λ_{max} of I-O (in nm)[a]

		PBE0		MLR, eq 1	
side	position	CN	NH_2	CN	NH_2
indoline	R_3	500	510	553	591
	R_4	494	511	562	567
	R_5	502	527	562	612
	R_6	495	501	561	576
naphthooxazine	$R_{5'}$	521	488	614	535
	$R_{6'}$	540	477	636	531
	$R_{7'}$	499	525	591	564
	$R_{8'}$	504	551	602	611
	$R_{9'}$	506	500	601	548

[a] All results have been obtained with PBE0 or eq 1 using cyclohexane as solvent.

obtained when the cyano group is in the vicinity of the ketone with significant displacements for 5′ (+32 nm) and 6′ (+54 nm), whereas 8′ (+20 nm) and 9′ (+19 nm) substitutions appear less efficient. The largest effect is clearly reached with an acceptor group at 6′, in perfect agreement with the experimental trends noted in Table 1. Adding a donor group (NH_2) on the naphthooxazine side may yield both bathochromic (positions 3 and 5) or hypsochromic (positions 4 and 6) shifts the largest impact being obtained at R_5 with an improvement of +30 nm. One would expect that placing the amino group on the opposite side of the photochrom would tune the λ_{max} toward smaller wavelengths. This is actually the case for all positions (5′, −47 nm; 6′, −51 nm; 7′, −27 nm; and 9′, −34 nm), except for 8′, for which we foresee a strong bathochromic effect (+29 nm). To our knowledge, the use of a strong donor group at $R_{8'}$ has not been attempted experimentally previously.

To summarize our findings, we predict that the largest (next largest) bathochromic shifts can be attained by using a donor group at R_5 ($R_{8'}$) or an acceptor group at $R_{6'}$ ($R_{5'}$). To rationalize these findings, we have depicted the topology of the frontier orbitals of four relevant open SPO structures in Figure 4. Indeed, all transitions reported in Figure 4 correspond to HOMO-to-LUMO transitions, and it has been checked that the HOMO−LUMO electronic gap qualitatively follows the wavelength trends of this table. For the unsubstituted molecule, both occupied and virtual orbitals are similar to that of Figure 3, as expected. The largest density spots, apart from the central chromogen, are located at the 5 and 8′ carbon atoms for the HOMO and 5′ and 6′ carbon atoms for the LUMO. This observation straightforwardly explains the above findings. The addition of a donor group at R_5 or $R_{8'}$ unstabilizes the HOMO, whereas acceptor groups located at 5′ and 6′ stabilize the LUMO. Both modifications yield a smaller electronic gap and therefore a larger λ_{max}. This explanation is further justified by the topology of the frontier orbitals for the $R_{6'}$ = CN and R_5 = NH_2 photochromes (Figure 4). Indeed, the HOMO of 6′-CN-**I-O** is completely like that of the unsubstituted molecule, whereas the LUMO is partly delocalized on the side group. The reverse situation occurs for 5-NH_2-**I-O**: significant modifications with respect to **I-O** are only to be noted for the HOMO.

Design of New Structures. As stated in the Introduction, our aim is to obtain SPO derivatives absorbing as close as possible from the IR domain. A reasonable chemical strategy is to combine the most effective positions (see previous section) for the donor and acceptor groups to develop new push−pull photochromes. We have therefore computed the λ_{max} of all possible open SPO built with the $R_{5'}$ = CN, $R_{6'}$ = CN, R_5 = NH_2, and $R_{8'}$ = NH_2 groups. Results are shown in Table 5.

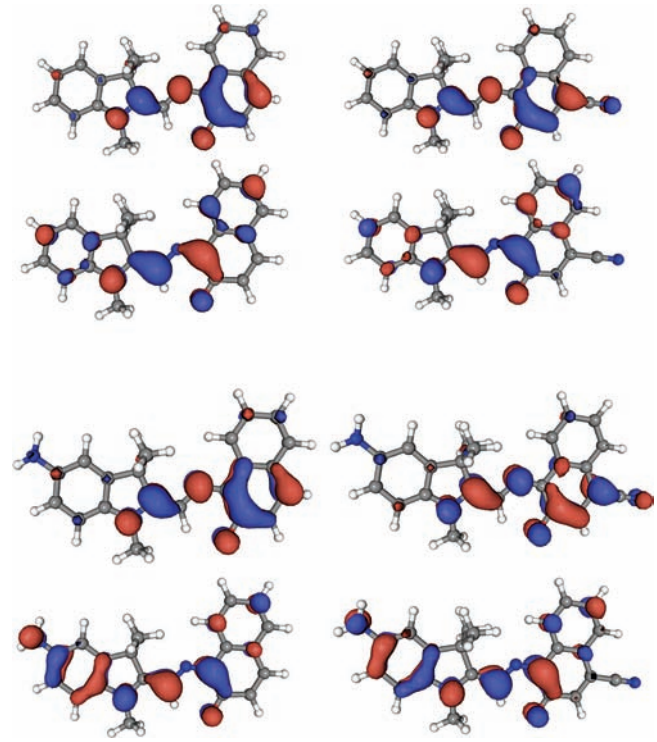

Figure 4. Frontier orbitals (PBE0, contour threshold of 0.04 au) calculated for unsubstituted **I-O** (top left), 6′-CN-**I-O** (top right), 5-NH_2-**I-O** (bottom right), and 5-NH_2,6′-CN-**I-O** (bottom right). For each compound, the HOMO (LUMO) is depicted at the bottom (top).

TABLE 5: Prediction of the λ_{max} (in nm) for Polysubstituted I-O[a]

substitution	PBE0	MLR, eq 1
none	499	582
$R_{5'}$ = CN	521	614
$R_{6'}$ = CN	540	636
R_5 = NH_2	527	612
$R_{8'}$ = NH_2	551	611
$R_{5'}$ = CN, $R_{6'}$ = CN	575	676
$R_{5'}$ = CN, R_5 = NH_2	553	640
$R_{5'}$ = CN, $R_{8'}$ = NH_2	584	663
$R_{6'}$ = CN, R_5 = NH_2	571	665
$R_{6'}$ = CN, $R_{8'}$ = NH_2	624	698
R_5 = NH_2, $R_{8'}$ = NH_2	566	635
$R_{5'}$ = CN, $R_{6'}$ = CN, R_5 = NH_2	612	701
$R_{5'}$ = CN, $R_{6'}$ = CN, $R_{8'}$ = NH_2	680	763
$R_{5'}$ = CN, R_5 = NH_2, $R_{8'}$ = NH_2	600	689
$R_{6'}$ = CN, R_5 = NH_2, $R_{8'}$ = NH_2	636	723
$R_{5'}$ = CN, $R_{6'}$ = CN, R_5 = NH_2, $R_{8'}$ = NH_2	693	789

[a] See Table 4 for more details.

First let us note that the general trends are similar with PBE0 and the MLR procedure, though the former seems to overestimate the auxochromic effects.

For the doubly substituted systems, the impact of the two auxochromes is almost additive, except with the $R_{8'}$ = NH_2 group, which appears to present an *enhancing* effect when combined with a cyano group. For instance, the λ_{max} of $R_{5'}$ = CN, $R_{6'}$ = CN ($R_{5'}$ = CN, R_5 = NH_2) is +94 nm (+58 nm) larger than its unsubstituted counterpart, whereas from the data of Table 4, one would have predicted +86 nm (+62 nm). As expected, the photochrome with two donor groups delivers the smallest absorption wavelength (635 nm) of the doubly substituted systems reported in Table 4, though it remains in line with the R_5 = OMe, $R_{6'}$ = CN reference SPO (650 nm, see Table 1). The largest displacement is obtained when placing the push

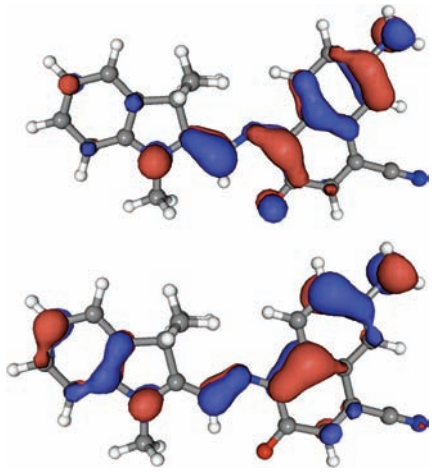

Figure 5. HOMO (bottom) and LUMO (top) of 8′-NH_2,6′-CN-**I-O**.

and pull moiety on the same side of the molecule, that is, with $R_{6'} = CN$ and $R_{8'} = NH_2$. Such a pattern delivers an estimated λ_{max} of 698 nm, i.e., significantly larger than the one obtained with the traditional push−pull patterns such as $R_{5'/6'} = CN$ and $R_5 = NH_2$. This 698 nm value is larger than any of the experimental value reported in Table 1. We also highlight that, on the sole basis of the λ_{max}, such a molecule seems to outperform the very large SPO recently proposed by Minkovska and co-workers,[70] though such a statement has certainly to be checked experimentally. Of course, an efficient SPO should conserve its photochromic efficiency and absorb in the UV part of the spectra in the closed form. To get first insights, additional analysis have been carried out. First, the topology of the frontier orbitals of 8′-NH_2,6′-CN-**I-O** related to its 698 nm absorption is given in Figure 5. As can be seen, compared to the usual 5-NH_2,6′-CN-**I-O** pattern reported in Figure 4, the main differences are (1) the absence of electron density on the carbonyl oxygen of the HOMO, (2) the apparently negligible impact of the cyano group for the LUMO, and (3) the large contribution of the top aromatic rings for both orbitals. Despite these variations, one notes that the carbon and oxygen atoms that should form the spiro bond (as well as atoms in the vicinity) still bear a significant contribution for the LUMO, so that Figure 5 does not rule out the possibility of photochromic closure. For the closed form, we have not designed a specific model, so that we have to rely on raw TD-DFT values to estimate if the absorption takes place in the UV or visible domain of the electromagnetic spectrum. As large errors may be associated with such raw TD-DFT values for the present molecules, we believe that only relative evolutions are relevant. For the unsubstituted closed form (**I-C**), the two first excited-states are located at 380 nm ($f = 0.07$) and 339 nm ($f = 0.17$) with TD-PBE0 in cyclohexane. For 5-NH_2,6′-CN-**I-C** SPO, a molecule similar to the one experimentally shown to develop photochromism, the same approach predicts significant bathochromic shifts for both peaks: 536 nm ($f = 0.06$) and 368 nm ($f = 0.23$). For the newly proposed 8′-NH_2,6′-CN-**I-C**, TD-PBE0 yields 435 nm ($f = 0.06$) and 424 nm ($f = 0.12$). Although the latter molecule may appear borderline from that criteria (a strong absorption above 400 nm), the variations with respect to the reference substitution pattern do not clearly indicate a general bathochromic shift: only the second transition undergoes such an effect. We are well aware that these simple considerations are certainly not absolute and should be confirmed by adequate experimental measurements, though this work hints that the synthesis of the 8′-NH_2,6′-CN-SPO derivative might be worth the effort!

Although few experiments have been carried out with three or more auxochromes added on the SPO core, the results of Table 4 confirm that such strategy may be efficient. Indeed, we foresee that one of the trisubstituted photochromes ($R_{5'} = CN$, $R_{6'} = CN$, $R_{8'} = NH_2$) as well as the tetrasubstituted SPO ($R_{5'} = CN$, $R_{6'} = CN$, $R_5 = NH_2$, $R_{8'} = NH_2$) would present their λ_{max} clearly positioned in the IR region: 763 and 789 nm, respectively. It is of course possible that such molecules would be unstable or undergo some of the practical problems noted above. While the investigation of these aspects with higher-level theoretical tools is beyond the scope of this initial investigation, it appears that the design of SPO derivatives with an open form absorbing in the IR domain is doable and probably deserves renewed attention.

Conclusions

Using a time-dependent density functional theory approach relying on the selection of large basis sets and the systematic modeling of solvent effects, we have assessed the structures and properties of SPO photochromes. A methodological investigation demonstrated that the 6-311+G(2d,p)//6-311G(d,p) basis set combination provides converged absorption wavelength when bulk solvent effects are included during all simulation steps. Due to the merocyanine nature of the open SPO structures, no DFT functional provides satisfactory results from both the qualitative and quantitative point of view. Subsequently, multiple linear regressions have been designed for cyclohexane and toluene. These equations provide mean absolute deviation of 6 and 4 nm, respectively, with large correlation coefficients, allowing an accurate and reliable design of new compounds. It turned out that plugging acceptor groups at the 5′ and 6′ positions of the naphthooxazine side provides a large bathochromic shift that can be further enhanced with the addition of donor groups at each side (5 and 8′) of the molecule. Using a double substitution on one side of the molecule, namely $R_{6'} = CN$, $R_{8'} = NH_2$, we predict a λ_{max} of nearly 700 nm, which is closer to the IR limit than any of the traditional SPO reported experimentally. Although many practical difficulties may impede the synthesis or practical use of such photochrom, we hope that this work will stimulate the synthesis of SPO presenting a donor group at $R_{8'}$.

Additionally, the investigation of the four most stable isomers of SPO revealed that only TTC and CTC conformers might occur experimentally for the open form, TTT and CTT isomers presenting Gibbs free energies larger by about 8.0 kcal mol^{-1} whatever the solvent and substituents selected. The two most stable conformers are within 1.5 kcal mol^{-1} of each other and present very similar absorption characteristics, i.e. they are unlikely to be distinguished by the sole use of the UV/vis spectroscopy.

Acknowledgment. D.J. and E.A.P. thank the Belgian National Fund for Scientific Research for their respective positions. All authors thank the Commissariat Général aux Relations Internationales and the Egide agency for supporting this work within the framework of the Tournesol Scientific cooperation between France and the Communauté Française de Belgique. Several calculations have been performed on the Interuniversity Scientific Computing Facility (ISCF), installed at the Facultés Universitaires Notre-Dame de la Paix (Namur, Belgium), for which the authors gratefully acknowledge the financial support of the FNRS-FRFC and the "Loterie Nationale" for the convention number 2.4578.02, and of the FUNDP.

Supporting Information Available: Tables describing the basis set, solvent effect, and functional methodological informations as well as a comparison between XRD and PBE0 geometries for the closed SPO form. This material is available free of charge via the Internet at http://pubs.acs.org.

References and Notes

(1) Dürr, H.; Bouas-Laurent, H. *Photochromism: Molecules and Systems*; Elsevier: New York, 2003.
(2) Delbaere, S.; Bochu, N. C.; Azaroual, N.; Buntinx, G.; Vermeersch, G. *J. Chem. Soc., Perkin Trans. 2* **1997**, 1499–1502.
(3) Aubard, J.; Maurel, F.; Buntinx, G.; Guglielmetti, R.; Levi, G. *Mol. Cryst. Liq. Cryst.* **2000**, *345*, 203–208.
(4) Maurel, F.; Aubard, J.; Rajzmann, M.; Guglielmetti, R.; Samat, A. *J. Chem. Soc., Perkin Trans. 2* **2002**, 1307–1315.
(5) Samat, A.; Lokshin, V. In *Organic Photochromic and Thermochromic Compounds*; Crano, J. C., Guglielmetti, R., Eds.; Plenum: New York, 1999; Vol. 2, pp 415−466.
(6) Betelson, R. C. In *Photochromism: Techniques of Chemistry*; Brown, G., Ed.; Wiley-Interscience: New York, 1971; pp 45−431.
(7) Chu, N. Y. C. In *Photochromism: Molecules and Systems*; Durr, H., Bouas-Laurent, H., Eds.; Elsevier: Amsterdam, 1990; Chapter 10, pp 493−508.
(8) Guglielmetti, R. In *Photochromism: Molecules and Systems*; Durr, H., Bouas-Laurent, H., Eds.; Elsevier: Amsterdam, 1990; pp 314−465.
(9) Maeda, S. In *Organic Photochromic and Thermochromic Compounds*; Crano, J. C., Guglielmetti, R., Eds.; Plenum: New York, 1999; Vol. 1, pp 85−109.
(10) Bertelson, R. C. In *Organic Photochromic and Thermochromic Compounds*; Crano, J. C., Guglielmetti, R., Eds.; Plenum: New York, 1999; Vol. 1, pp 11−73.
(11) Day, D.; Gu, M.; Smallridge, A. In *Infrared Holography for Optical Communications: Techniques, Materials and Devices*; Boffi, P., Piccinin, D., Ubaldi, M. C., Eds.; Springer-Verlag: Berlin, 2003; Chapter 1, pp 1−18.
(12) Lokshin, V.; Samat, A.; Metelitsa, A. V. *Russ. Chem. Rev.* **2002**, *71*, 893–916.
(13) Metelitsa, A. V.; Lokshin, V.; Micheau, J. C.; Samat, A.; Guglielmetti, R.; Minkin, V. I. *Phys. Chem. Chem. Phys.* **2002**, *4*, 4340–4346.
(14) Voloshin, N. A.; Metelitsa, A. V.; Micheau, J. C.; Voloshina, E. N.; Besugliy, S. O.; Vdovenko, A. V.; Shepelin, N. E.; Minkin, V. I. *Russ. Chem. Bull., Int. Ed.* **2003**, *52*, 1172–1181.
(15) Metelitsa, A. V.; Micheau, J. C.; Besugliy, S. O.; Gaeva, E. B.; Voloshin, N. A.; Voloshina, E. N.; Samat, A.; Minkin, V. I. *Int. J. Photoenergy* **2004**, *6*, 199–204.
(16) Nakamura, S.; Uchida, K.; Murakami, A.; Irie, M. *J. Org. Chem.* **1993**, *58*, 5543–5545.
(17) Horii, T.; Abe, Y.; Nakao, R. *J. Photochem. Photobiol. A: Chem.* **2001**, *144*, 119.
(18) Maurel, F.; Aubard, J.; Millie, P.; Dognon, J.; Rajzmann, M.; Guglielmetti, R.; Samat, A. *J. Phys. Chem. A* **2006**, *110*, 4759–4771.
(19) Maurel, F.; Samat, A.; Guglielmetti, R.; Aubard, J. *Mol. Cryst. Liq. Cryst.* **2000**, *345*, 75–80.
(20) Dreuw, A.; Head-Gordon, M. *Chem. Rev.* **2005**, *105*, 4009–4037.
(21) Barone, V.; Polimeno, A. *Chem. Soc. Rev.* **2007**, *36*, 1724–1731.
(22) Goerigk, L.; Moellmann, J.; Grimme, S. *Phys. Chem. Chem. Phys.* **2009**, *11*, 4611–4620.
(23) Jacquemin, D.; Perpète, E. A.; Ciofini, I.; Adamo, C. *Acc. Chem. Res.* **2009**, *42*, 326–334.
(24) Jacquemin, D.; Perpète, E. A. *Chem. Phys. Lett.* **2006**, *429*, 147–152.
(25) Perrier, A.; Maurel, F.; Aubard, J. *J. Photochem. Photobiol. A: Chem.* **2007**, *189*, 167–176.
(26) Perpète, E. A.; Maurel, F.; Jacquemin, D. *J. Phys. Chem. A* **2007**, *111*, 5528–5535.
(27) Mançois, F.; Pozzo, J. L.; Pan, J.; Adamietz, F.; Rodriguez, V.; Ducasse, L.; Castet, F.; Plaquet, A.; Champagne, B. *Chem.—Eur. J.* **2009**, *15*, 2560–2571.
(28) Jacquemin, D.; Perpète, E. A.; Scalmani, G.; Frisch, M. J.; Assfeld, X.; Ciofini, I.; Adamo, C. *J. Chem. Phys.* **2006**, *125*, 164324.
(29) Petit, L.; Quartarolo, A.; Adamo, C.; Russo, N. *J. Phys. Chem. B* **2006**, *110*, 2398–2404.
(30) Adamo, C.; Barone, V. *J. Chem. Phys.* **1999**, *110*, 6158–6170.
(31) Ernzerhof, M.; Scuseria, G. E. *J. Chem. Phys.* **1999**, *110*, 5029–5036.
(32) Perdew, J. P.; Burke, K.; Ernzerhof, M. *Phys. Rev. Lett.* **1996**, *77*, 3865–3868.
(33) Tao, J.; Perdew, J.; Staroverov, V.; Scuseria, G. *Phys. Rev. Lett.* **2003**, *91*, 146401.
(34) Staroverov, V. N.; Scuseria, G. E.; Tao, J.; Perdew, J. P. *J. Chem. Phys.* **2003**, *119*, 12129–12137.
(35) Baker, J.; Pulay, P. *J. Chem. Phys.* **2002**, *117*, 1441–1449.
(36) Becke, A. D. *J. Chem. Phys.* **1993**, *98*, 5648–5652.
(37) Stephens, P. J.; Devlin, F. J.; Chabalowski, C. F.; Frisch, M. J. *J. Phys. Chem.* **1994**, *98*, 11623–11627.
(38) Zhao, Y.; Schultz, N. E.; Truhlar, D. G. *J. Chem. Phys.* **2005**, *123*, 161103.
(39) Boese, A. D.; Martin, J. M. L. *J. Chem. Phys.* **2004**, *121*, 3405–3416.
(40) Becke, A. D. *J. Chem. Phys.* **1993**, *98*, 1372–1377.
(41) Zhao, Y.; Truhlar, D. G. *Acc. Chem. Res.* **2008**, *41*, 157–167.
(42) Tomasi, J.; Mennucci, B.; Cammi, R. *Chem. Rev.* **2005**, *105*, 2999–3094.
(43) Cossi, M.; Barone, V. *J. Chem. Phys.* **2001**, *115*, 4708–4717.
(44) *Statgraphics Plus 5.1.*; Manugistics Inc.: Herndon, VA, 2000.
(45) Jacquemin, D.; Preat, J.; Charlot, M.; Wathelet, V.; André, J. M.; Perpète, E. A. *J. Chem. Phys.* **2004**, *121*, 1736–1743.
(46) Perpète, E. A.; Wathelet, V.; Preat, J.; Lambert, C.; Jacquemin, D. *J. Chem. Theory Comput.* **2006**, *2*, 434–440.
(47) Jacquemin, D.; Wathelet, V.; Preat, J.; Perpète, E. A. *Spectochim. Acta A* **2007**, *67*, 334–341.
(48) Parac, M.; Grimme, S. *J. Phys. Chem. A* **2002**, *106*, 6844–6850.
(49) Dierksen, M.; Grimme, S. *J. Chem. Phys.* **2004**, *120*, 3544–3554.
(50) Santoro, F.; Improta, R.; Lami, A.; Bloino, J.; Barone, V. *J. Chem. Phys.* **2007**, *126*, 084509.
(51) Improta, R.; Barone, V.; Scalmani, G.; Frisch, M. J. *J. Chem. Phys.* **2006**, *125*, 054103.
(52) Perpète, E. A.; Jacquemin, D. *J. Photochem. Photobiol. A: Chem.* **2007**, *187*, 40–44.
(53) Laurent, A. D.; André, J. M.; Perpète, E. A.; Jacquemin, D. *Chem. Phys. Lett.* **2007**, *436*, 84–88.
(54) Jacquemin, D.; Perpète, E. A. *Chem. Phys. Lett.* **2006**, *420*, 529–533.
(55) Jacquemin, D.; Wathelet, V.; Perpète, E. A. *J. Phys. Chem. A* **2006**, *110*, 9145–9152.
(56) Jacquemin, D.; Perpète, E. A.; Scalmani, G.; Frisch, M. J.; Kobayashi, R.; Adamo, C. *J. Chem. Phys.* **2007**, *126*, 144105.
(57) Jacquemin, D.; Perpète, E. A.; Scuseria, G. E.; Ciofini, I.; Adamo, C. *J. Chem. Theory Comput.* **2008**, *4*, 123–135.
(58) Iikura, H.; Tsuneda, T.; Yanai, T.; Hirao, K. *J. Chem. Phys.* **2001**, *115*, 3540–3544.
(59) Yanai, T.; Tew, D. P.; Handy, N. C. *Chem. Phys. Lett.* **2004**, *393*, 51–56.
(60) Toulouse, J.; Colonna, F.; Savin, A. *Phys. Rev. A* **2004**, *70*, 062505.
(61) Vydrov, O. A.; Heyd, J.; Krukau, V.; Scuseria, G. E. *J. Chem. Phys.* **2006**, *125*, 074106.
(62) Peach, M. J. G.; Benfield, P.; Helgaker, T.; Tozer, D. J. *J. Chem. Phys.* **2008**, *128*, 044118.
(63) Schreiber, M.; Bub, V.; Fülscher, M. P. *Phys. Chem. Chem. Phys.* **2001**, *3*, 3906–3912.
(64) Görner, H. *Chem. Phys. Lett.* **1998**, *282*, 381–390.
(65) Görner, H. *Phys. Chem. Chem. Phys.* **2001**, *3*, 416–423.
(66) Benard, S.; Pei, Y. *Chem. Commun.* **2000**, 65–66.
(67) Leaustic, A.; Dupont, A.; Yu, P.; Clement, R. *New. J. Chem.* **2001**, *25*, 1297–1301.
(68) Millini, R.; Del Piero, G.; Allegrini, P.; Crisci, L.; Malatesta, V. *Acta Crystallogr. C* **1991**, *47*, 2567–2569.
(69) Favaro, G.; Masetti, F.; Mazzucato, U.; Ottavi, G.; Allegrini, P.; Malatesta, V. *J. Chem. Soc. Faraday Trans.* **1994**, *90*, 333–338.
(70) Minkovska, S.; Jeliazkova, B.; Borisova, E.; Avramov, L.; Deligeorgiev, T. *J. Photochem. Photobiol. A: Chem.* **2004**, *163*, 121.

JP906936P